

# Rhodanine-Based Tau Aggregation Inhibitors in Cell Models of Tauopathy\*\*

Bruno Bulic, Marcus Pickhardt, Inna Khlistunova, Jacek Biernat, Eva-Maria Mandelkow, Eckhard Mandelkow,\* and Herbert Waldmann\*

The two histopathological hallmarks that characterize Alzheimer's disease (AD) are the extracellular amyloid plaques that are formed by  $\beta$ -amyloid fragments of the amyloid precursor protein (APP), and intracellular neurofibrillary tangles and neuropil threads, which consist of the microtubule-associated protein tau forming paired helical filaments with highly ordered structures, as recently corroborated by X-ray microcrystallography.<sup>[1]</sup> In addition, tau deposits similar to those of AD occur in several "tauopathies".<sup>[2,3]</sup> The normal function of tau is to stabilize the microtubule network for the transport of vesicles and organelles in nerve cells, which is necessary for the communication between cells and thus for brain activity. When tau aggregates, it is thought that the tracks for transport (microtubules) break down and the transport is interrupted.<sup>[4–6]</sup> Moreover, the relevance of tau for neurodegeneration induced by  $\beta$  amyloid has been demonstrated in a mouse model.<sup>[7,8]</sup> It would therefore be highly desirable to find methods to keep tau in a functional state and prevent or reverse abnormal aggregation. The quest for cures for Alzheimer's disease is very intense. Available therapies to date make use of cholinesterase inhibitors and NMDA receptor antagonists,<sup>[9,10]</sup> and newer approaches focus, for

example, on inhibition of tau phosphorylation and aminopeptidase activation.<sup>[11–14]</sup>

Thus, the development of tau aggregation inhibitors that are also able to disaggregate filaments could provide an alternative to existing strategies.<sup>[15–18]</sup> Herein we report the investigation of substituted rhodanines with these properties in vitro and in a cell model consisting of a neuroblastoma cell line that expresses tau in an inducible fashion with subsequent aggregation. In an initial high-throughput screen,<sup>[19,20]</sup> several aggregation inhibitors were identified. From these hits, rhodanines (2-thioxothiazolidin-4-ones, Figure 1 a) were

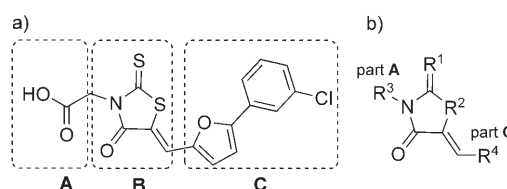


**Figure 1.** Variation of inhibitor structure. a) Structure of the hit compound. Variations of flanking regions of the central rhodanine core (part B) are possible in parts A and C. b) Variations of the core (R<sup>1</sup> and R<sup>2</sup>) and on the flanking substituents (R<sup>3</sup> and R<sup>4</sup>).

selected for synthesis of a collection because of their activity in the screening and because the rhodanine core in general has been shown to be a viable scaffold for the development of biologically active molecules. Thus, rhodanines are classified as nonmutagenic,<sup>[21]</sup> and a long-term study on the clinical effects of the rhodanine-based Epalrestat demonstrated that it is well tolerated.<sup>[22]</sup> Several assays were performed to develop compounds that would show strong effects on the assembly and disassembly of paired helical filaments (characterized by their IC<sub>50</sub> and DC<sub>50</sub> values, corresponding to the half maximal compound concentration necessary for inhibition of tau assembly into aggregates and disassembly of preformed filament aggregates, respectively). We performed a tau aggregation assay in vitro based on the fluorescence change of the aggregate-specific stain thioflavin S (ThS) as a readout and using the three-repeat tau construct K19 derived from the fetal isoform htau23<sup>[19,23]</sup> (see the Supporting Information). In addition, we investigated the aggregation of the four-repeat construct K18, either with the wild-type sequence, or with two types of mutations. In the "proaggregation" mutant K18ΔK280, the absence of K280 strongly enhances aggregation.<sup>[24]</sup> The opposite behavior is observed with the "antiaggregation" mutant by the insertion of prolines, which act as breakers of  $\beta$  structure and thus prevent aggregation (I277P, I308P).<sup>[25]</sup>

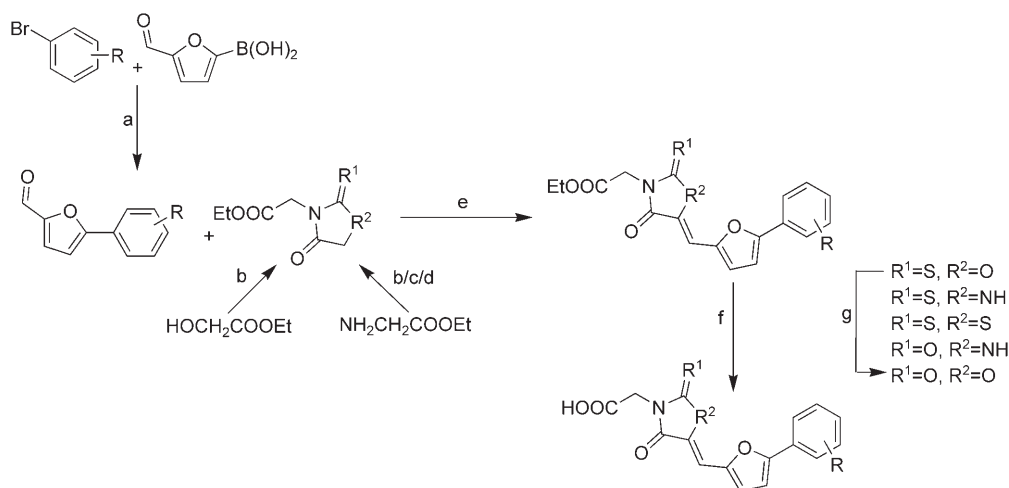
[\*] Dr. M. Pickhardt,<sup>[‡]</sup> Dr. I. Khlistunova, Dr. J. Biernat, Dr. E.-M. Mandelkow, Prof. E. Mandelkow  
Max-Planck-Unit for Structural Molecular Biology  
c/o DESY, Notkestrasse 85, 22607 Hamburg (Germany)  
Fax: (+49) 408-971-6810  
E-mail: mand@mpasmb.desy.de  
Dr. B. Bulic,<sup>[‡]</sup> Prof. H. Waldmann  
Max-Planck-Institute for Molecular Physiology  
Otto-Hahn-Strasse 11, 44227 Dortmund (Germany)  
and  
Center for Applied Chemical Genomics  
Otto-Hahn-Strasse 15, 44227 Dortmund (Germany)  
E-mail: herbert.waldmann@mpi-dortmund.mpg.de  
and  
Universität Dortmund, Fachbereich 3  
Otto-Hahn-Strasse 6, 44227 Dortmund (Germany)  
Fax: (+49) 231-1332499

[‡] These authors contributed equally to this work.

[\*\*] This work was supported in part by grants from the Deutsche Forschungsgemeinschaft (DFG), the Institute for the Study of Aging (ISOA), the European Union ("Europäischer Fond für regionale Entwicklung"), and the state of North Rhine-Westphalia. We thank Sabrina Hübschmann and Ilka Lindner for excellent technical assistance.

Supporting information for this article (synthesis and characterization data) is available on the WWW under <http://www.angewandte.org> or from the author.

For the synthesis of a compound collection we employed an iterative approach and focused on the heterocycle as well as its substituents. Initial attempts focused on immobilization of an *N*-carboxyalkyl-substituted rhodanine core on a polymeric resin by means of an ester bond, and subsequent Knoevenagel reaction with aromatic aldehydes equipped with a suitable functional group to allow formation of the biaryl bond by means of a Pd<sup>0</sup>-catalyzed aryl coupling reaction. However, these attempts failed because the Pd<sup>0</sup>-catalyzed reaction was inhibited by the rhodanine heterocycle. Thus, the solution-phase synthesis sequence shown in Scheme 1 was



**Scheme 1.** Synthesis of a compound collection. Reagents: a) 5 mol % [PdCl<sub>2</sub>(PPh<sub>3</sub>)<sub>2</sub>], 2 M aq Na<sub>2</sub>CO<sub>3</sub>, 1,2-dimethoxyethane, 85 °C, 9 h. b) Ethyl isothiocyanatoacetate, Et<sub>3</sub>N, toluene, reflux, 4 h. c) Bis(carboxymethyl)tri-thiocarbonate, Na<sub>2</sub>CO<sub>3</sub>, *i*PrOH, reflux, 18 h. d) Bis(*p*-nitrophenyl)carbonate, Et<sub>3</sub>N, *N,N*-dimethylformamide, room temperature, 12 h then HCl aq, dioxane, reflux, 2 h. e) For R<sup>2</sup> = O, NH: NaOAc, dioxane, 90 °C, 2 h; for R<sup>2</sup> = S: piperidine, CH<sub>2</sub>Cl<sub>2</sub>, room temperature, 12 h. f) NaOH, dioxane/water, room temperature, 1 h. g) *meta*-Chloroperoxybenzoic acid, NaHCO<sub>3</sub>, CH<sub>2</sub>Cl<sub>2</sub>, room temperature, 24 h.

employed; this sequence involves formation of biaryl aldehydes and subsequent Knoevenagel condensation with the rhodanine core as key steps (for a solid-phase synthesis of rhodanines by a different strategy, see reference [28]). The aryl aldehydes necessary for the Knoevenagel condensation (part C, Figure 1a) were obtained by Suzuki coupling between haloaromatics and functionalized boronic acids (Scheme 1).

Initially, we focused on the central heterocycle itself, replacing the original rhodanine core with other heterocycles (R<sup>1</sup> and R<sup>2</sup>, Figure 1b). In these experiments, rhodanines (R<sup>1</sup> = S and R<sup>2</sup> = S), thiohydantoin (R<sup>1</sup> = S and R<sup>2</sup> = N), thioxooxazolidine (R<sup>1</sup> = S and R<sup>2</sup> = O), oxazolidinedione (R<sup>1</sup> = O and R<sup>2</sup> = O), and hydantoin (R<sup>1</sup> = O and R<sup>2</sup> = N) were employed (see the Supporting Information) and the following trend in inhibition of tau aggregation was observed: rhodanine (**1**) > thiohydantoin (**3**) > oxazolidinedione (**7**) > thioxooxazolidinone (**9**) > hydantoin (**10**). The rhodanine heterocycle appeared to be the most potent. The thioxo group in rhodanines is known as a carboxylic acid bioisoster by size, low electronegativity, and ability to build hydrogen bonds.<sup>[26,27]</sup> On the basis of these observations, the rhodanine

heterocycle was kept, and substituents A and C were varied (Figure 1a).

We investigated the importance of the carboxylic acid (A, Figure 1a) and the influence of the substitution and length of the linker connecting the central core (B, Figure 1a) to the carboxylic acid (Figure 2). Replacement of the carboxylic acid with an imidazole or a benzimidazole as well as esterification led to reduced disassembly activity (Table 1, entries 1–4). Furthermore, the length of the linker between the carboxylic acid and the rhodanine core (B, Figure 1a) was varied. These experiments revealed that increasing the

distance up to two carbon bonds resulted in an appreciable increase in the compound's inhibitory potency without markedly affecting the disassembly activity (Table 1, entries 1, 5, and 6). In subsequent experiments, biaryl part C of the compounds (Figure 1a) was varied. The heteroaromatic side chain (part C, Figure 1a) tolerated variations, but modifications on the furan heterocycle led to reduced potency (Table 1, entries 1, 5, and 7–9, and the Supporting Information), probably as a result of both electronic and steric changes, as replacement of the furan ring in **16** for thiophene in **22** reduced the potency. Very bulky substituents, such as adamantyl or ferrocene (Table 1, entries 10 and 11), at the end of side chain C were generally well tolerated, reducing the overall efficiency of the compounds only slightly. Also, introduction of a charged group by means of a carboxylic acid did not influence the potency considerably (Table 1, entries 12–14), underlining the structural flexibility around this position.

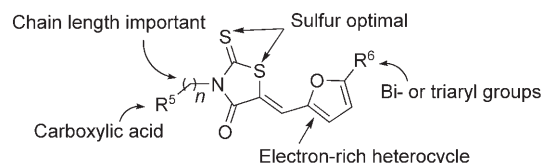


**Figure 2.** Structure–activity relationship.

After completing the synthesis of our focused library, we observed that the efficiency of the most potent derivatives are in the nanomolar range for both inhibition and disaggregation (**19**, IC<sub>50</sub> = 0.17 μM, DC<sub>50</sub> = 0.13 μM, Table 1). Examples of dose–response curves are shown in Figure 3, both for the

**Table 1:** Compound structures, IC<sub>50</sub> and DC<sub>50</sub> values, PHF inhibition in cells, and cytotoxicity.

Entry	Compd	R <sup>3</sup> <sup>[a]</sup>	R <sup>4</sup> <sup>[a]</sup>	IC <sub>50</sub> [μM] <sup>[b]</sup>	DC <sub>50</sub> [μM] <sup>[b]</sup>	Inhibition in cells <sup>[c]</sup> [%]
1	1			0.82	0.10	20.40 ± 5.37
2	4			4.36	1.80	n.d.
3	14			0.67	0.94	70.47 ± 4.49
4	49			1.09	0.80	n.d.
5	16			0.47	0.30	21.55 ± 13.82
6	23			1.22	1.04	n.d.
7	22			0.97	0.77	n.d.
8	27			5.03	1.66	n.d.
9	42			7.92	1.40	n.d.
10	44			0.69	0.42	n.d.
11	54			0.37	0.47	n.d.
12	33			0.58	0.52	n.d.
13	34			0.73	0.60	n.d.
14	35			0.78	0.58	n.d.
15	30			0.26	0.16	69.02 ± 3.10
16	17			0.54	0.39	62.67 ± 4.08
17	19			0.17	0.13	16.49 ± 4.38

[a] Substituents  $R^3$  and  $R^1$  refer to Figure 1 b ( $R^1 = R^2 = S$ ). [b] The  $IC_{50}$  and  $DC_{50}$  values represent the assembly-inhibition and disassembly-inducing half-maximal concentrations, respectively, measured in vitro. For each data point, experiments were performed in triplicate and averaged. The standard error of the  $IC_{50}$  or  $DC_{50}$  values determined from the curves was 10–20%. [c] The values obtained by incubating the cells with 15  $\mu M$  compound correspond to the level of inhibition of tau aggregation normalized to a control without inhibitor (0%) in cells. n.d.: not determined.

inhibition of aggregation (Figure 3 a) and for the dissolution of preformed paired helical filaments (PHFs; Figure 3 b).

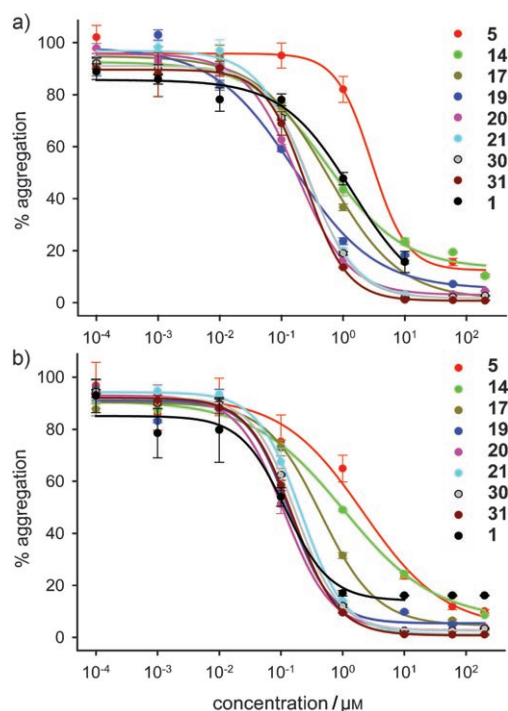
The curves exhibit the typical sigmoidal decrease of aggregated protein at increasing compound concentrations.

Figure 4 illustrates examples of PHFs, made from the construct K19, in the process of disassembly after incubation overnight with increasing inhibitor concentrations of **30**. Filaments are seen in various stages of shortening or breaking and reveal a concentration-dependent degree of dissolution.

The compounds were investigated in murine neuroblastoma N2a cells to determine whether they are also active in cellular systems. In these experiments, tau expression was induced by incubation with doxycyclin. The results shown in Figure 5 were obtained by switching on the tau expression by doxycyclin, incubating the cells with compound (15  $\mu\text{M}$ ), and scoring for ThS fluorescence after 5 days. To assess the depolymerization of pre-formed aggregates, the expression of tau was induced for 5 days, then compounds were added, and the level of ThS fluorescence was measured after 2 more days. In these experiments the compounds were applied in 15  $\mu\text{M}$  concentration because they were not cytotoxic to the cells at this concentration (see below).

To exclude that the cell assay results might be impaired by potential cytotoxicity of the aggregation inhibitors, all compounds were assayed for cytotoxicity at 10  $\mu$ M concentration. Orientating experiments employed an established lactate dehydrogenase assay (LDH), which reports on the leakiness of membranes in degenerating cells. After the cells were incubated for 24 hours with 10  $\mu$ M compound, the degree of cell lysis was determined by LDH release. The assay revealed that the compounds are not or at worst only very weakly cytotoxic (see the Supporting Information).<sup>[19,29]</sup> Furthermore, we investigated whether some of the most potent compounds interfere with the physiological function of tau, that is, binding to microtubules.

An in vitro assay of tubulin polymerization or absence of **14** and **30**, which was used to confirm the specificity in the cellular assay (inhibition of polymerization relative to the untreated control) showed that the IC<sub>50</sub> of **14** was 50  $\mu$ M (i.e. four times higher than the



**Figure 3.** Dose–response curves. a) Inhibition of tau aggregation by rhodanine-derived compounds. The extent of aggregation is measured by ThS fluorescence and plotted as a percentage of the untreated control. The black line represents the initial hit structure **1**. b) Dose–response curves for disassembly of preformed PHFs by rhodanine-derived compounds.

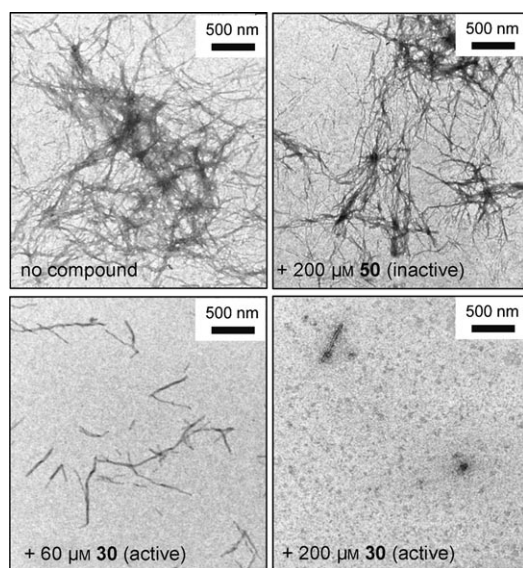


**Figure 4.** Electron micrographs of K19 PHFs treated with different concentrations of **30** and **50** for 12 h at 37°C, showing the breakdown of PHFs into smaller fragments for compound **30**. Inactive compound **50** was used for a negative control. The methods used are described elsewhere.<sup>[6]</sup>

concentration used in the cellular screen), revealed that tubulin polymerization is at most only marginally affected by the rhodanines. In this established assay, tubulin at 30  $\mu\text{M}$

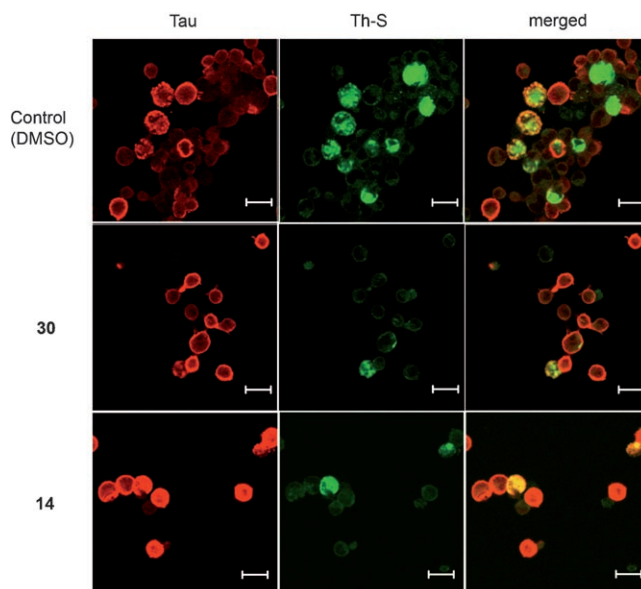


**Figure 5.** Cell assay of aggregation inhibitors. Expression of K18 $\Delta$ K280 tau in doxycycline-inducible N2a cells leads to aggregate formation, which is inhibited by rhodanines. Cells were stained with aggregate-specific thioflavine-S (green, center column) and with tau antibody K9JA (red, left column). Compounds **30** and **14** were applied for 5 days at 15  $\mu\text{M}$  (top row, without inhibitor; middle row, with **30**; bottom row, with **14**). Note the disappearance of the ThS stain relative to the control without compound (“DMSO”). Scale bar: 20  $\mu\text{m}$ .

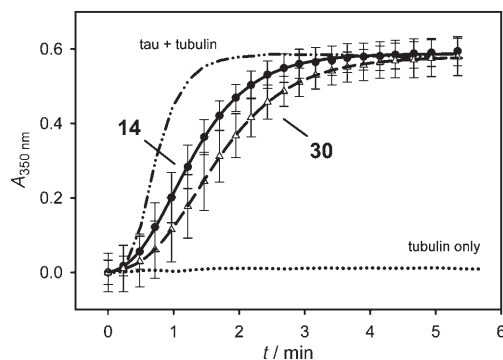


**Figure 6.** Rhodanines have only a minor effect on tau-induced microtubule assembly. Tubulin dimer (30  $\mu\text{M}$ ) was incubated with hTau40wt (10  $\mu\text{M}$ ) in the presence or absence of rhodanine compounds (60  $\mu\text{M}$ ). Samples were incubated in a microtiter plate at 37°C, and absorption was measured continuously at 350 nm and plotted versus time. Tubulin alone ..... tubulin and hTau40wt ----, rhodanine **14** —●—, and rhodanine **30** —△—.

without tau served as a negative control because it is unable to self-assemble into microtubules below the critical concentration. In the presence of tau (10  $\mu\text{M}$ ), tubulin polymerizes within 4 minutes (Figure 6).<sup>[19]</sup>

Taken together, these results demonstrate that the rhodanines investigated by us inhibit tau aggregation and most importantly promote paired helical filament disassembly at 100–600 nm concentration. They also display activity in cellular assays without showing cytotoxicity (at the concentration investigated) or interference with the normal function



of tau to promote tubulin polymerization. The initial structure-determining properties of the inhibitors observed in vitro, which do not fully translate into the activities seen in the cellular context, may result from different penetration through the cell membrane. Nonetheless, our data suggest that the compound class identified by us may hold substantial promise for further development.

Compounds that induce disaggregation of already formed PHFs, prevent aggregation or in the best scenario combine both properties are of particular interest for medicinal chemistry research focusing on AD.

Received: September 3, 2007

Published online: November 5, 2007

**Keywords:** aggregation inhibitors · Alzheimer's disease · medicinal chemistry · neurochemistry · tau proteins

- [1] M. R. Sawaya et al., *Nature* **2007**, 447, 453–457; see the Supporting Information. The fact that paired helical filaments have a highly ordered core has been shown before, for example, by X-ray diffraction; see references [25], [30], and [31].
- [2] V. M. Lee, J. Q. Trojanowski, *J. Alzheimer's Dis.* **2006**, 9, 257–262.
- [3] L. Buée, T. Bussiere, V. Buee-Scherrer, A. Delacourte, P. R. Hof, *Brain Res. Rev.* **2000**, 33, 95–130.
- [4] A. Ebner, R. Godemann, K. Stamer, S. Illenberger, B. Trinczek, E. Mandelkow, *J. Cell Biol.* **1998**, 143, 777–794.
- [5] K. Stamer, R. Vogel, E. Thies, E. Mandelkow, E. M. Mandelkow, *J. Cell Biol.* **2002**, 156, 1051–1063.
- [6] E. M. Mandelkow, E. Thies, B. Trinczek, J. Biernat, E. Mandelkow, *J. Cell Biol.* **2004**, 167, 99–110.
- [7] E. D. Roberson, K. Searce-Levie, J. J. Palop, F. Yan, I. H. Cheng, T. Wu, H. Gerstein, G. Q. Yu, L. Mucke, *Science* **2007**, 316, 750–754.
- [8] B. Bandyopadhyay, G. Li, H. Yin, J. Kuret, *J. Biol. Chem.* **2007**, 282, 16454–16464.
- [9] A. Martinez, A. Castro, *Expert Opin. Invest. Drugs* **2006**, 15, 1–12.
- [10] R. A. Hansen, G. Gartlehner, K. N. Lohr, D. I. Kaufer, *Drugs Aging* **2007**, 24, 155–167.
- [11] S. L. Karsten et al., *Neuron* **2006**, 51, 549–560; see the Supporting Information.
- [12] S. Le Corre et al., *Proc. Natl. Acad. Sci. USA* **2006**, 103, 9673–9678; see the Supporting Information.
- [13] W. Noble et al., *Proc. Natl. Acad. Sci. USA* **2005**, 102, 6990–6995; see the Supporting Information.
- [14] K. S. Hung, S. L. Hwang, C. L. Liang, Y. J. Chen, T. H. Lee, J. K. Liu, S. L. Hwang, C. H. Wang, *J. Neuropathol. Exp. Neurol.* **2005**, 64, 15–26.
- [15] C. M. Wischik, P. C. Edwards, R. Y. Lai, M. Roth, C. R. Harrington, *Proc. Natl. Acad. Sci. USA* **1996**, 93, 11213–11218.
- [16] C. Chirita, M. Necula, J. Kuret, *Biochemistry* **2004**, 43, 2879–2887.
- [17] S. Taniguchi, N. Suzuki, M. Masuda, S. Hisanaga, T. Iwatsubo, M. Goedert, M. Hasegawa, *J. Biol. Chem.* **2004**, 280, 7614–7623.
- [18] C. E. Augelli-Szafran (Warner Lambert Co), WO0076988, **2000**.
- [19] a) M. Pickhardt, Z. Gazova, M. von Bergen, I. Khlistunova, Y. P. Wang, A. Hascher, J. Biernat, E. M. Mandelkow, E. Mandelkow, *J. Biol. Chem.* **2004**, 280, 3628–3635. In this paper, anthraquinones are described as tau aggregation inhibitors. However, this compound class is significantly more cytotoxic than the rhodanines described herein; b) M. Pickhardt, G. Larbig, I. Khlistunova, A. Coksezen, B. Meyer, E. M. Mandelkow, B. Schmidt, E. Mandelkow, *Biochemistry* **2007**, 46, 10016–10023. The described phenylthiazolylhydrazides display comparable activity in cellular assay but a lower biochemical potency.
- [20] M. Pickhardt, M. von Bergen, Z. Gazova, A. Hascher, J. Biernat, E. M. Mandelkow, E. Mandelkow, *Curr. Alzheimer Res.* **2005**, 2, 219–226.
- [21] E. Zeiger, B. Anderson, S. Haworth, T. Lawlor, K. Mortelmans, W. Speck, *Environ. Mutagen.* **1987**, 9, 1–110.
- [22] N. Hotta et al., *Diabetes Care* **2006**, 29, 1538–1544; see the Supporting Information.
- [23] P. Friedhoff, A. Schneider, E. M. Mandelkow, E. Mandelkow, *Biochemistry* **1998**, 37, 10223–10230.
- [24] S. Barghorn, Q. Zheng-Fischhofer, M. Ackmann, J. Biernat, M. von Bergen, E. M. Mandelkow, E. Mandelkow, *Biochemistry* **2000**, 39, 11714–11721.
- [25] M. von Bergen, P. Friedhoff, J. Biernat, J. Heberle, E. M. Mandelkow, E. Mandelkow, *Proc. Natl. Acad. Sci. USA* **2000**, 97, 5129–5134.
- [26] G. A. Patani, E. J. LaVoie, *Chem. Rev.* **1996**, 96, 3147–3176.
- [27] S. Miyamoto, *Chem-Bio Inf. J.* **2002**, 2, 74–85.
- [28] C. H. Lee, M. M. Sui, *Tetrahedron Lett.* **2000**, 41, 5729–5732.
- [29] I. Khlistunova, J. Biernat, Y. P. Wang, M. Pickhardt, M. von Bergen, Z. Gazova, E. Mandelkow, E. M. Mandelkow, *J. Biol. Chem.* **2005**, 281, 1205–1214.
- [30] M. von Bergen, S. Barghorn, L. Li, A. Marx, J. Biernat, E. M. Mandelkow, E. Mandelkow, *J. Biol. Chem.* **2001**, 276, 48165–48174.
- [31] J. Berriman, L. C. Serpell, K. A. Oberg, A. L. Fink, M. Goedert, R. A. Crowther, *Proc. Natl. Acad. Sci. USA* **2003**, 100, 9034–9038.
- [32] A. J. Leo, *Chem. Rev.* **1993**, 93, 1281–1306.